X-ray scattering studies of charge-density waves in tantalum disulfide

L. D. Chapman* and R. Colella
Department of Physics, Purdue University, West Lafayette, Indiana 47907
(Received 21 September 1984)

The temperature dependence of the wave vectors and intensities of the charge-density-wave satellites in 1 T-TaS_2 have been investigated in detail in the noncommensurate (NC) and incommensurate (IC) phases with the use of x-ray precession photography and counter measurements. In the IC phase ($T \geq 80$°C) the intensities of first-order satellites are found to vary smoothly, and have led to the establishment of a "phason temperature factor." In the NC phase, temperature-dependent domain structures have been found which prevent quantitative studies as a function of temperature. Second- and higher-order satellites are found to be, at room temperature, several orders of magnitude more intense than the values predicted by the simple sinusoidal model. It is suggested that in the NC phase several harmonics are present, which, however, disappear in the IC phase. It is found that in this phase the sinusoidal model is well applicable.

I. INTRODUCTION

The basic problem addressed in this work is in the general area of thermal excitations of a modulated structure; more specifically, the effect of temperature on satellite reflections arising from charge-density waves (CDW's).[-1] The effect of phonons on Bragg reflections is well known. Each structure factor is attenuated by the Debye-Waller factor e^{-M}. When CDW's are present, Overhauser predicted several years ago the existence of a new kind of low-energy excitation, called "phasons," which should give rise to a similar kind of temperature factor acting on satellite reflections only.[2] The problem one encounters in experiments of this kind is that when temperature is changed, as for example in the experiments described in Ref. 3, CDW amplitudes and wave vectors change as well, making it difficult or impossible to disentangle effects due to thermal vibrations only, as distinct from those arising from changes in the structure of CDW's. It is like trying to verify the theory of the Debye-Waller factor in diffraction by measuring diffracted intensities as a function of temperature in a crystal in the neighborhood of a structural phase transition.

Inelastic neutron scattering studies of molecular crystals such as byphenyl (Ref. 4) and $ThBr_4$ (Ref. 5) have revealed the existence of temperature-dependent excitations that have been interpreted as phase and amplitude modes. Given the complexity of lattice dynamics in molecular crystals, it is difficult to arrive at unequivocal identification of all vibrational modes.

Temperature effects on CDW satellites and phase-phase correlations have been discussed in neutron scattering studies on KCP [$K_2Pt(Cn)_4Br_{03}\cdot nH_2O$],[6] a one-dimensional system, in relation to broadening of CDW peaks with increasing temperature. The fact that the size of coherent domains is temperature dependent makes it difficult to understand in simple terms the effect and the nature of thermal excitations in a modulated structure such as KCP.

Transition-metal dichalcogenides crystallize in layered structures with two-dimensional properties. Among the various examples of crystals exhibiting CDW's, transition-metal dichalcogenides are probably the best systems for studying the physics of modulated structures, owing to their good quality, chemical stability, and relatively easy availability. The satellite reflections resulting from periodic modulations in their lattice constants are well visible in all diffraction experiments with x rays, neutrons, and electrons, and all results are well reproducible.

Structural information is best obtained from elastic diffraction experiments. X rays have advantages over neutrons because the available beams from laboratory sources have much more intensity at comparable resolution, a critical factor when only small and very thin samples are available, as is the case of TaS_2, $TaSe_2$, and the like. Furthermore, the extinction problem and the effect of multiple scattering are less severe with x rays, owing to higher absorption and the falling off of the scattering factors with k, the momentum exchanged in the scattering process. Given the high intensity available, a small incident beam can be used, the longest dimension of the cross section being typically 1 mm or less, with the advantage that a small area of the crystal is utilized, which allows a better control of the domain structure of the CDW's. More importantly, with a beam smaller than the crystal, all intensity measurements can be put on an absolute basis, which greatly increases the amount of information extractable from diffraction experiments. These advantages are normally not available in typical neutron scattering experiments, in which the beam has ordinarily a cross section much larger than that of the crystal.

With respect to electron diffraction, the resolution in k space is not as good as with x rays, especially along directions parallel to the c^* axis, owing to the small thickness of the crystals perpendicular to the c axis. More importantly, intensity information is not readily available due to multiple-beam effects, which are overwhelming in electron-diffraction patterns. The only real advantage of electron diffraction is the possibility of obtaining photographic images of planar cross sections of reciprocal space

intersecting the origin, which allows fast and direct determination of CDW wave vectors. In surveying reciprocal space, the advantage of the photographic method over the lengthier procedure of point-by-point counter scanning is obvious. However, one caution must be exercised in interpreting electron-diffraction patterns because some of the spots may correspond to nonexisting CDW's, as a result of multiple-beam effects.

To overcome these problems, we decided to make use of an equivalent photographic technique for x rays: namely, precession photography, which gives on film an undistorted view of a planar section of reciprocal space, not necessarily intersecting the origin. The idea is to use precession photography as a preliminary technique for fast and accurate characterization of CDW wave vectors on various $(h\,k\,\zeta)$ planes ($\zeta=0,\frac{1}{6},\frac{1}{3},\ldots,1$), and then proceed with more accurate quantitative counter measurements.

We decided to concentrate on $1T$-TaS_2, which exhibits well-developed CDW's at room temperature. The main thrust of this work, as stated at the beginning of this section, is to investigate the temperature dependence of CDW satellites. Since $1T$-TaS_2 exhibits a polymorphic phase transition at 80 °C,[7,8] which only involves the CDW system not the underlying crystalline structure, it was not clear at the beginning what the most convenient temperature range should be for our investigations. We decided for practical reasons to confine our studies to the range 25—150 °C, well below the limit $T\simeq 175$ °C, above which the CDW's disappear.

The strategy of this work has been to perform initially a thorough exploration of the reciprocal lattice, using the precession method, at different temperatures. We then focused on a limited number of first- and higher-order satellites, corresponding to a relatively wide range of the scattering vector, and performed accurate point-by-point scans using a three-circle counter spectrometer. We found that the physics of the incommensurate $1T_1$ structure ($T>80$ °C) is much more understandable than that of the noncommensurate $1T_2$ structure ($T<80$ °C). Interesting results have been obtained, however, in both ranges of temperatures, and results will be presented for both structures.

II. EXPERIMENTAL TECHNIQUES AND RESULTS

A suitable TaS_2 crystal was selected from a batch grown at Purdue, in the Central Materials Preparation Facility, following well-known procedures.[9] The crystal was about $5\times4\times0.0398$ mm^3 in volume. The thickness was evaluated from the absorption factor for Mo $K\alpha$ radiation, using published values for the absorption coefficient,[10] and was found to be uniform over the area utilized for our measurements. The crystal was mounted in a small furnace, equipped with Mylar windows, that could be safely operated up to 150 °C. The inside atmosphere was air at normal pressure, which caused a slight oxidation on the surface of the crystal, a yellowish color, of no consequence.

A precession camera was equipped with a flat graphite monochromator, and mounted at the exit port of an Elliott 15-kW (nominal) rotating-anode x-ray generator. The precession camera was mounted on a rotating table, and the monochromator crystal could be translated out of the beam, so that the white beam could be utilized for orientation purposes. Photographs were taken of different layers $(h\,k\,\zeta)$, with $\zeta=0,\pm\frac{1}{6},\pm\frac{1}{3},\pm\frac{1}{2}$ at 25, 50, 75, 85, 120 and 150 °C. Typical conditions were 30 kV, 250 mA, for 15 h. The excitation voltage was kept low in order to avoid $\lambda/2$ spots.

For quantitative measurements a conventional x-ray generator and a sealed x-ray tube (maximum power 1.8 kW) were utilized, in conjunction with a curved quartz monochromator. The beam (Mo$K\alpha$) was converging with an angle of 0.8° on the axis of the spectrometer, with a vertical divergence of about 0.5°. The beam size, at the crystal, was about 1×0.2 mm^2. Since the beam was completely intercepted by the crystal, all measurements of integrated intensities could be put on an absolute basis. The incident-beam intensity was electronically stabilized to $\pm0.1\%$, and the power of the primary beam was periodically measured before and after each integrated intensity measurement by using a set of calibrated filters as attenuators. The background was evaluated on both sides of the diffraction peaks, and subtracted by using a linear extrapolation under the peak. An ω-2θ spectrometer (Huber), with limited χ rotation ($\pm45°$), equipped with a scintillation counter and a single-channel analyzer, was used under computer control. All measurements were done with the c axis in the scattering plane. It is known that the basic set of first-order CDW satellites in TaS_2 form a rhombohedral sublattice.[7] We found, in agreement with the results of Ref. 7, that at room temperature (RT) the magnitude Q of a first-order CDW satellite wave vector is 0.112 Å^{-1}, and the angle α of the rhombohedral sublattice is 59.9°. The three basic wave vectors $\mathbf{Q}_1$, $\mathbf{Q}_2$, and $\mathbf{Q}_3$ form equal angles with the c axis of the crystal, and the c component Q_c is equal to $\frac{1}{3}c^*$. Each Bragg reflection on the $(h\,k\,0)$ plane is accompanied by three first-order satellite reflections located on the $(h\,k\,\frac{1}{3})$ plane, $+\mathbf{Q}_1,+\mathbf{Q}_2,\mathbf{Q}_3$, and three symmetrically located satellites on the $(h\,k\,-\frac{1}{3})$ plane, $-\mathbf{Q}_1,-\mathbf{Q}_2,-\mathbf{Q}_3$. We call $\mathbf{Q}_3$ the wave vector whose component $\mathbf{Q}_3^0$ on the $(h\,k\,0)$ plane forms the smallest angle, in magnitude, with the reciprocal-lattice vector $\mathbf{G}$ of the parent Bragg reflection associated to $\mathbf{Q}_1$, $\mathbf{Q}_2$, and $\mathbf{Q}_3$. The order in which the satellites are numbered is anticlockwise as seen from the $+c^*$ direction. The angle ϕ between $\mathbf{Q}_3^0$ and $-\mathbf{G}$ is about 10.9° for the $1T_2$ phase, and zero for the $1T_1$.

Figure 1 is the $(h\,k\,0)$ layer at room temperature. Only second- and higher-order satellites can be seen on this layer. The photograph of Fig. 1, as well as all other photographs, have been carefully analyzed using computer-simulated photographs with satellites of different orders. The heavy spots are Bragg reflections, strongly overexposed. The streaking is due to incomplete monochromaticity of the beam, and is different for the various spots. It is practically absent for those spots for which the nondispersive $(n,-n)$ double-crystal parallel arrangement is realized.[11] The spots visible in Fig. 1 are mostly second- and third-order satellites. Some weak fourth-order satellites are also visible.

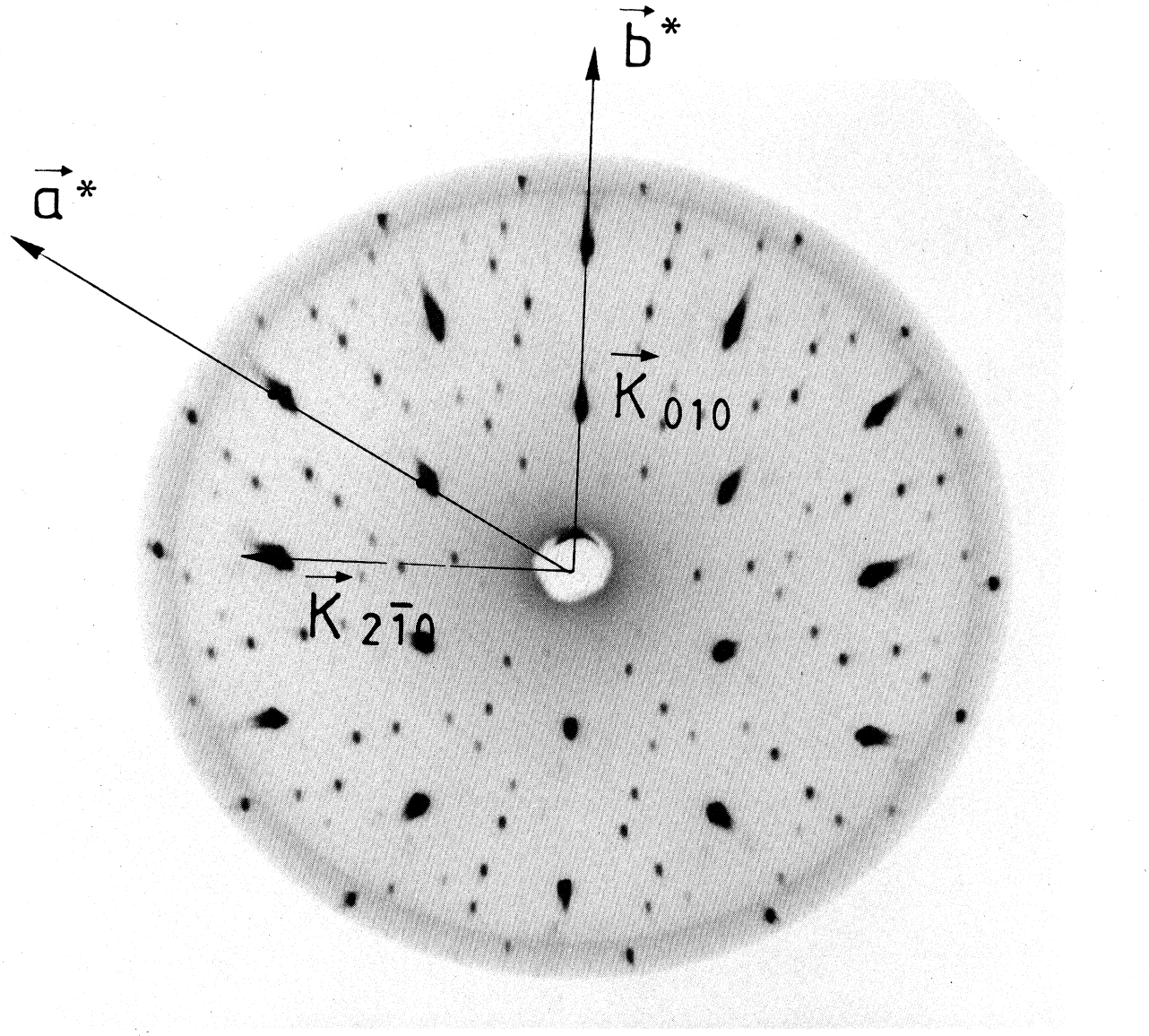

FIG. 1. Precession photograph of the (h k 0) layer at room temperature. Mo $K\alpha$ radiation. The heavy spots are Bragg reflections. Only second- and higher-order satellites are visible in this photograph.

Figure 2 shows the (h k $\frac{1}{3}$) layer at room temperature. The strongest satellites are first order. Three satellites associated with the same parent Bragg reflection (2$\bar{2}$0) are shown within the black circle. Sometimes one of the three satellites, in other areas of the photograph, is weak because the scattering vector is almost perpendicular to the displacements of the Ta and S atoms. Higher-order satellites are also well visible, up to third order. In some cases the room-temperature photographs showed two different kinds of CDW's, which will be called α and β. This was an indication of two different kinds of equivalent domains, in which the angle ϕ had different signs. Care was taken to select a position on the crystal in which only one kind was present. In some instances, however, it was found that the percentage of one kind of domain with respect to the other was temperature dependent. This is dramatically evident in Fig. 3, which shows a complicated spot pattern.

Figure 3 is the (h k $\frac{1}{3}$) layer at 50 °C. A careful comparison with Fig. 2 shows that the crystal region explored by the x-ray beam, which was entirely in the α phase at room temperature, changed mostly, but not entirely, to the β phase. This phenomenon was very noticeable at 50 °C. At 75 °C (Fig. 4) the ϕ angle is reduced to zero, so that the α and β phases coincide, and the higher-order satellites have vanished, which is even more evident in Fig. 5, showing the (h k 0) layer at 75 °C. All satellites are now gone, and the thermal diffuse scattering is enhanced, as expected. This disappearance of the higher-order satellites and the vanishing of the ϕ angle are no doubt related

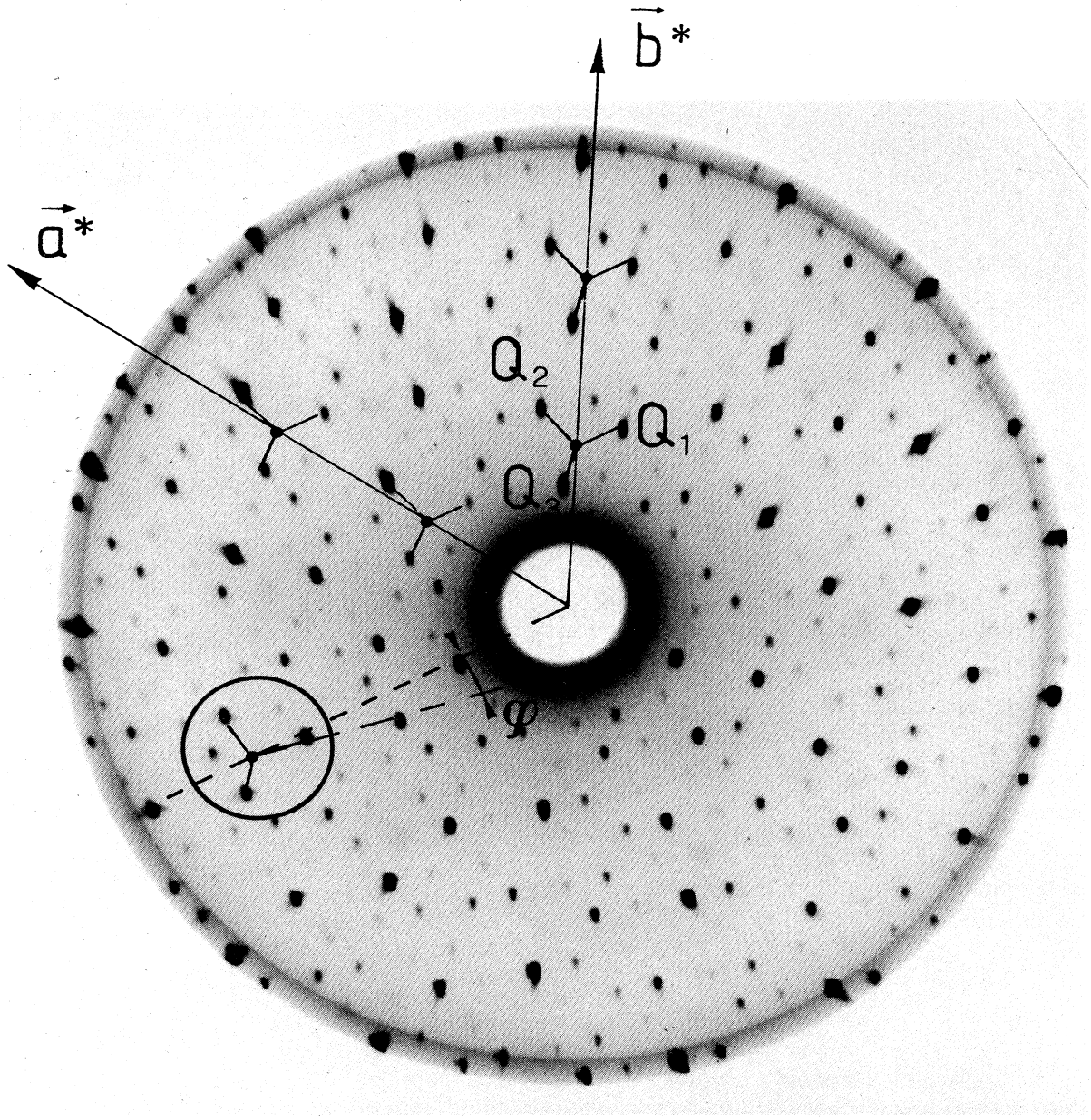

FIG. 2. Precession photograph of the $(h\ k\ \frac{1}{3})$ layer at room temperature. The triplet enclosed by a black circle (heavy spots) corresponds to a set of three first-order satellites associated with the (020) Bragg reflection. Higher-order satellites (up to third order) are visible.

to the onset of the incommensurate phase ($1T_1$), which, however, takes place sharply at a higher temperature: 80 °C. Nothing dramatic happens in the photographs taken above 75 °C, so they will not be shown here.

The integrated intensities of several Bragg reflections and satellites of various orders have been measured with high accuracy (typically $\pm 1\%$) using a counter. The (010) and (030) were most likely affected by extinction and will not be discussed here.

The (0016) gave an interesting result. Its integrated intensity was only 43.7% of the expected value, computed *for a crystal without CDW's.*

The (0016), which was calculated using a Debye-Waller factor estimated from data published in Ref. 12 ($M = 1.237$ at 298 K), is a very weak reflection, and most likely not affected by extinction. The dynamical value[13] (valid for a perfect crystal) is only 14% less than the kinematic value (valid for a mosaic crystal). Therefore, the only explanation for the anomalously low experimental value is to assume that the CDW displacements have some components along the c axis (presumably for the sulfur atoms only). However, the experiments described

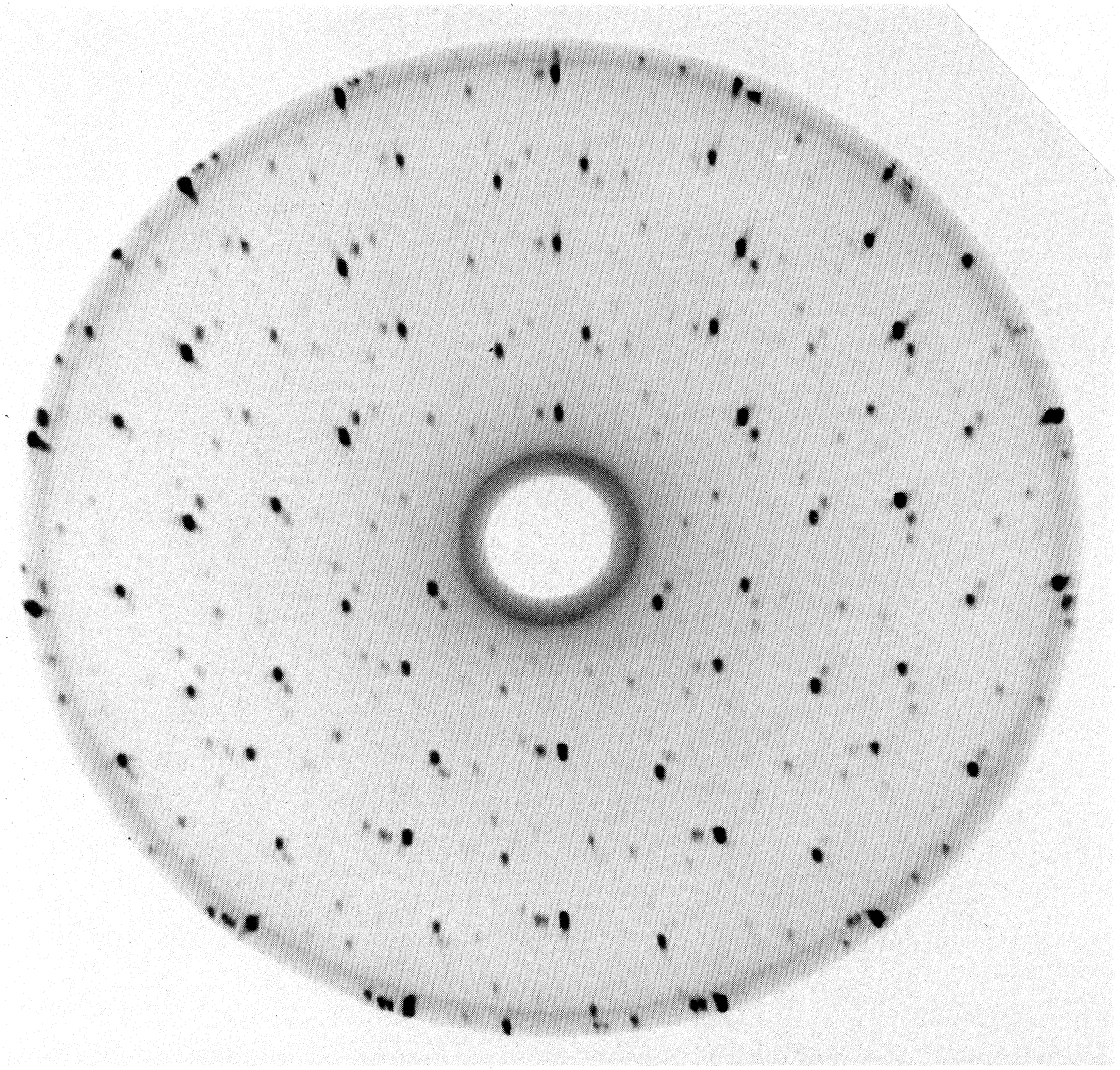

FIG. 3. Same as Fig. 2, except that $T=50\,°C$. Two sets of spots are visible, corresponding to two equivalent sets of CDW satellites, with opposite orientations around the c axis with respect to the main reciprocal lattice.

in Ref. 12 show that the $(0\,0\,l)$ reflections are not affected by the polymorphic $1T_2 \leftrightarrow 1T_1$ transition at 80 °C, as opposed to what happens for the $(0\,h\,0)$ and $(h\,h\,0)$ reflections. We are therefore led to draw the curious conclusion that, although the CDW displacements *have nonzero components* along the c axis, *only their components in the basal planes are allowed to change discontinuously at the* $1T_2 \leftrightarrow 1T_1$ *transition.* Presumably this result implies that only Ta atoms move along the basal planes at the transition. The CDW atomic displacements of the sulfur atoms are not affected.

A total of six first-order satellites have been measured quantitatively at different temperatures. Three of them (S_1,S_2,S_3) were associated with the (010) Bragg reflection, the other three (S_4,S_5,S_6) with the (030). Their temperature dependence between 90 and 150 °C was analyzed in detail in our preliminary report[14] and has led to the establishment of the existence of phasons.

The integrated intensity values at various temperatures are given in Table I, along with the values taken between RT and 70 °C. The latter set of values could not be analyzed in the same way as the data taken in the higher-temperature range (90—150 °C) because the intensity values did not vary smoothly in this range. *For this reason 25—90 °C data have not been plotted.* The reason for the irregular behavior of the $1T_2$ phase, below 80 °C, is undoubtedly due to the temperature-dependent domain formations α and β described earlier in this section. In Table I we also list the calculated values resulting from the fitting procedure described in Ref. 14. The fit is in

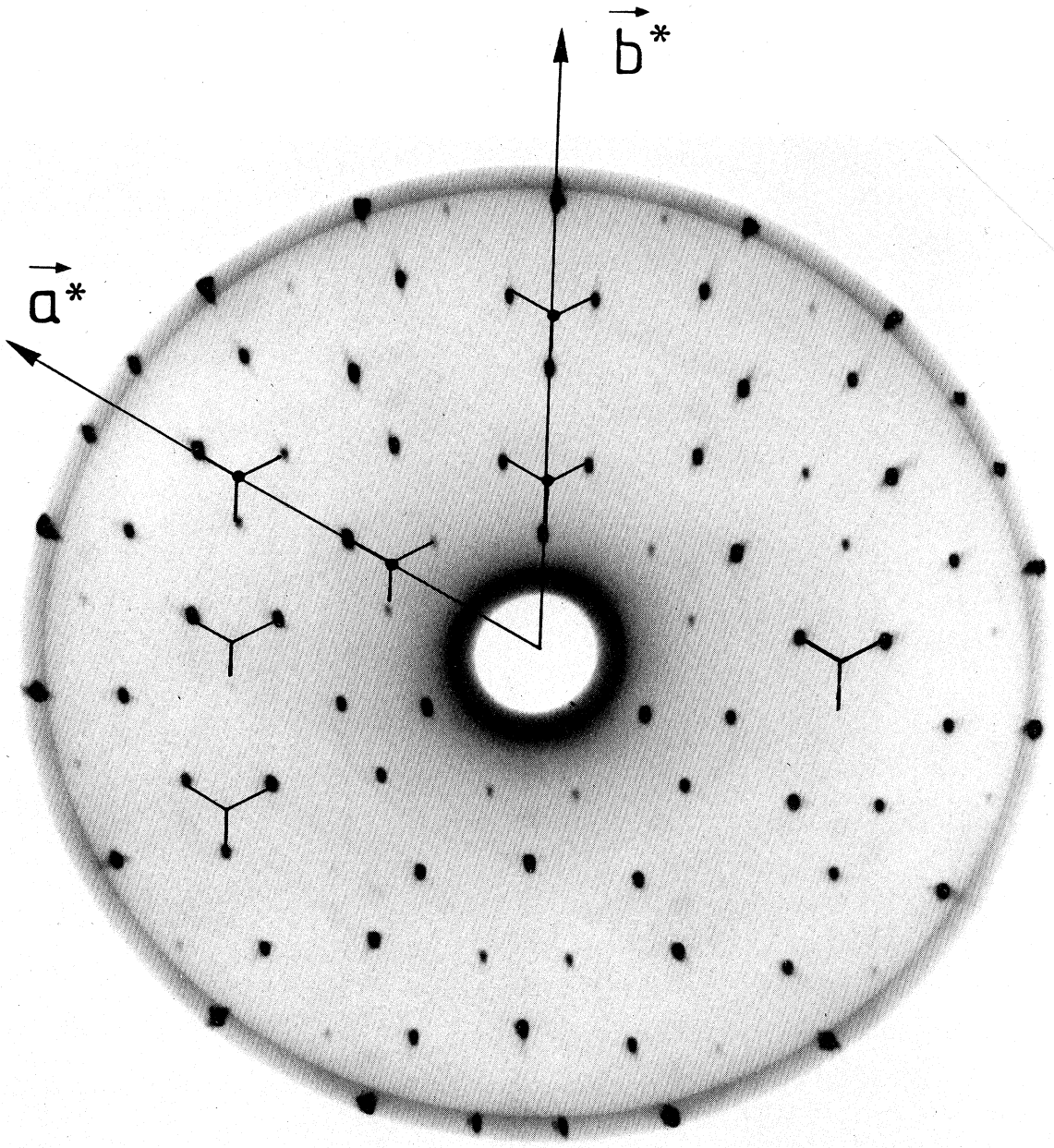

FIG. 4. Same as Fig. 2, except that $T=70\,^{\circ}\mathrm{C}$. Only first-order satellites are visible here. The crystal is still in $1T_2$ phase, but the CDW satellites system exhibits features that are typical of the $1T_1$ phase.

general very good, with R values ranging between 2.4% and 1.2%.

Some higher-order satellites have also been measured at various temperatures. Their values are given in Table II. What is immediately apparent from Table II is the large and sharp discontinuity of each intensity value across the $1T_2 \leftrightarrow 1T_1$ transition. Most satellites become too weak to be measured in the $1T_1$ phase, with the exception of satellite D.

III. DISCUSSION

Only data taken in the $1T_1$ phase have been found to be consistent with a simple sinusoidal model. The theory developed by Giuliani and Overhauser[15] for polyatomic crystals has been extended to the case of three equivalent

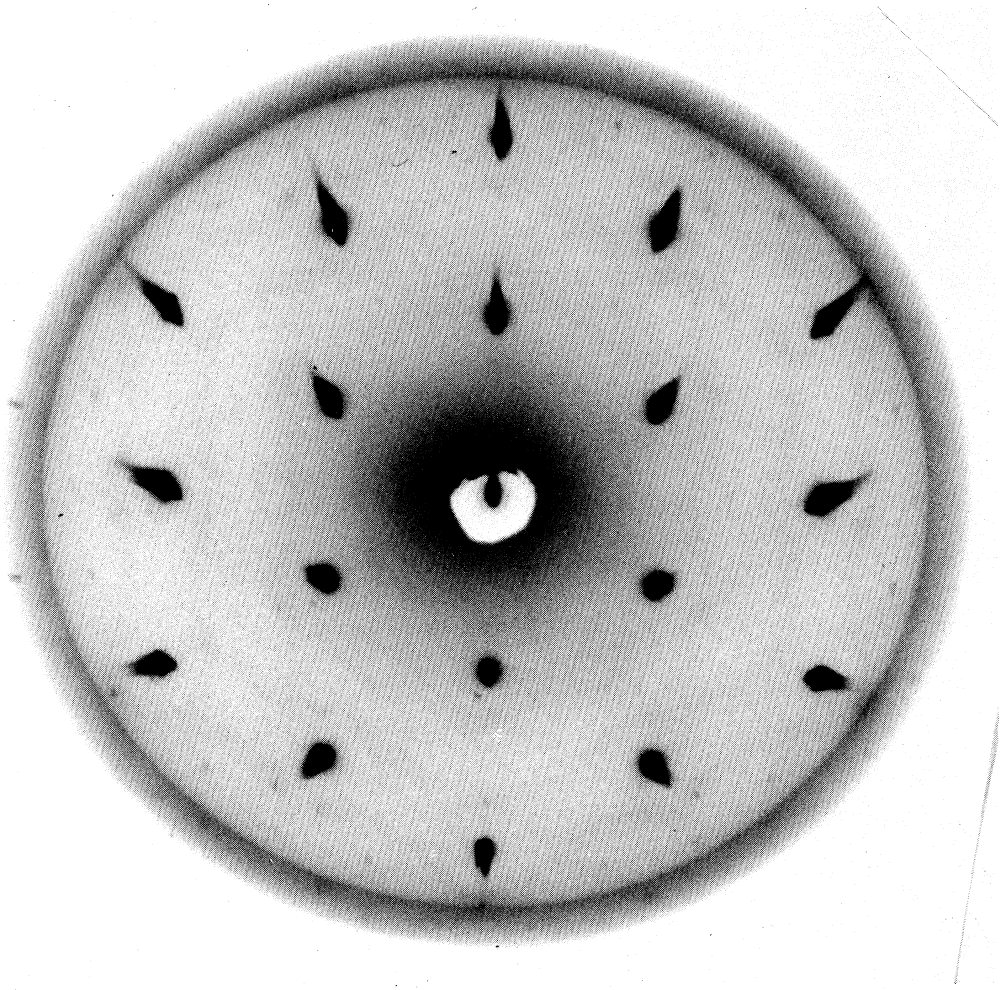

FIG. 5. Same as Fig. 4, except that here the (h k 0) plane is shown. No more satellites are visible, and the thermal diffuse scattering has increased.

TABLE I. Absolute integrated intensities of six first-order satellites at different temperatures. S_1,S_2,S_3 are associated to the (0 1 0) Bragg reflection. S_4,S_5,S_6 are associated to the (0 3 0). All values should be multiplied by 10^{-7}. In each box, the upper figure is the experimental value, the lower one is calculated from the fit described in Ref. 2. The percentage experimental error, based on statistics only, is less than $\pm 1\%$.

T (°C)	S_1	S_2	S_3	S_4	S_5	S_6
25	4.11	1.11	5.31	1.66	1.41	3.81
50	3.81	1.11	5.15	1.46	1.24	3.76
70	3.55	1.04	5.07	1.39	1.24	3.69
90	2.96	2.88	4.53	1.25	1.22	3.99
	2.85	2.98	4.55	1.18	1.28	3.99
110	2.75	2.79	4.21	1.16	1.14	3.55
	2.71	2.84	4.22	1.11	1.19	3.55
130	2.60	2.58	3.98	1.04	1.03	3.39
	2.56	2.63	3.99	1.01	1.05	3.39
150	2.44	2.47	3.65	0.970	0.984	3.08
	2.38	2.54	3.66	0.925	1.03	3.08

TABLE II. Absolute integrated intensities of six second- and higher-order satellites at different temperatures. The Miller indices *hkl* indicate the parent Bragg reflection of each satellite. The three integer numbers n_1,n_2,n_3 are the Miller indices of each satellite referred to the rhombohedral set of coordinates, in which the first-order satellites $\mathbf{Q}_1,\mathbf{Q}_2,\mathbf{Q}_3$ are the basic translation vectors. (See text, Sec. II.) All values should be multiplied by 10^{-9}. In each box the upper figure is the experimental value, the lower one is calculated using the displacement values obtained in the fit described in Ref. 2. The percentage experimental error, based on statistics only, is less than ±1%. Missing experimental values were too weak to be measured.

T (°C)	A	B	C	D	E	F
hkl	0 1 0	0 1 0	0 1 1	0 3 0	0 3 0	0 3 1
n_1,n_2,n_3	$0,\bar{1},1$	$1,\bar{1},1$	$0,\bar{3},0$	$0,\bar{1},1$	$1,\bar{1},1$	$0,\bar{3},0$
25	177	78.9	5.36	205	42.6	13.4
50	153	63.8	4.76	176	36.2	10.1
70	129	49.4	2.96	150	28.5	2.12
90				4.51		
	0.035	4.8×10^{-5}	6.9×10^{-10}	6.11	0.11	5.7×10^{-9}
110				4.00		
				4.90		
130				3.22		
				3.97		
150				2.03		
				3.79		

CDW's. The following expression has been obtained:

$$S(\mathbf{q})=\sum_i f_i(\mathbf{q})\exp[i(\tau_i\cdot\mathbf{G}+n_1\phi_{i1}+n_2\phi_{i2}+n_3\phi_{i3})]\times J_{n_1}(\mathbf{q}\cdot\mathbf{A}_{i1})J_{n_2}(\mathbf{q}\cdot\mathbf{A}_{i2})J_{n_3}(\mathbf{q}\cdot\mathbf{A}_{i3})\times\exp[-C(n_1^2+n_2^2+n_3^2)T]\,, \quad (1)$$

where $S(\mathbf{q})$ is the generalized structure factor, $\mathbf{q}$ is the scattering vector, corresponding to a given satellite specified by its three Miller indices n_1,n_2,n_3, $f_i(\mathbf{q})$ is the atomic scattering factor of the ith atom within the crystal cell,[16] whose location is given by τ_i originating from within the unit cell (typical of the CdI_2 structure), $\mathbf{G}$ is the reciprocal-lattice vector of the associated parent Bragg reflection, ϕ_{ij} is the phase, *a priori* unknown, of the jth CDW affecting the ith atom, J_{n_1},J_{n_2},J_{n_3} are Bessel functions of integer orders, and A_{ij} is the atomic displacement amplitude of the jth CDW affecting the ith atom. The order of the satellite is given by $|n_1|+|n_2|+|n_3|$. The last exponential factor is the "phason temperature factor" (PTF) discussed in Ref. 14. This expression takes place of the ordinary structure factor in the formula given by kinematic theory for the integrated intensity diffracted by a plane-parallel crystal plate in the Laue Case (Ref. 11, Chap. II, Sec. 2-h). The ordinary Debye-Waller factor has not been included because it is not known. The only value we know with a reasonable degree of accuracy is for $(0\,0\,l)$ reflections, but it is expected to be strongly anisotropic. In our preliminary report[14] we have explained in detail the fitting procedures that have allowed us to determine the free parameters of our model, namely longitudinal displacements for Ta (A_{Ta}), longitudinal and c displacements for S ($A_{\mathrm{S}}^{l},A_{\mathrm{S}}^{c}$), and phase angle between basal displacements of Ta and S atoms (ϕ_x). By "longitudinal displacements" we mean projections on the basal planes. The values determined in Ref. 14 are $A_{\mathrm{Ta}}=0.166\pm0.001$ Å, $A_S^l\cong0.0$ Å, $A_S^c=0.7$–0.8 Å, and $\phi_x\cong56°$, and are shown to be independent of temperature, so that all intensity changes at different temperatures could be explained by one single PTF. It was shown in Ref. 14 that the effect of the PTF was to reduce by a factor of 4 the intensities of all first-order satellites at 90 °C, contrary to the prediction of an alternate treatment of phason modes in modulated structures due to Axe,[17] in which no effect is expected for first-order satellites. A crystallographic refinement performed on Na_2Co_3 by Hogervorst, Peterse, and de Wolff,[18] is mentioned in Ref. 17 as possible support of the theoretical prediction given therein. Since a PTF of the form given in formula (1) acts with the same value on all satellites of the same order, it can be easily missed in a crystallographic refinement, in which all intensities are measured relative to one another, not on an absolute basis as in our work.

When those values for the displacements and phase, given in Ref. 14, are used to calculate the intensity of a second-order satellite (called D in Table II), agreement between theory and experiment is within 1 order of magnitude. The values between 90 and 130 °C are actually closer, within 25–30 %, which can be considered a fairly good agreement, given the experimental errors involved and the approximations of the theory, in particular, the neglect of the ordinary Debye-Waller factor. The value at 150 °C was very difficult to measure because the satellite was exceedingly weak. The experimental error is large be-

cause this satellite was on the wing of a strong and rapidly varying background of thermal diffuse scattering, presumably associated to a Bragg reflection. The striking features of Table II are the *unusually high values of all satellite intensities below 90*°C. The discontinuity of satellite D across the $1T_1 \leftrightarrow 1T_2$ transition amounts to a factor of 33. Most of the first-order satellites are, instead, more or less continuous across the transition, and it is not possible to explain the intensities of Table II below 90°C, even when some allowance is made for reasonable changes across the transition. The same PTF is assumed to be in operation at 90 and 70°C. If we compare the experimental intensities at 70°C with those calculated at 90°C, the discrepancies found range from a minimum factor of 25 for satellite D (second order) to a maximum factor of 4.3×10^9 for satellite C (third order). The net result of this analysis is that *in the $1T_2$ phase the higher-order satellites are much stronger than their expected values,* by several orders of magnitudes in some cases.

The only logical conclusion we are able to draw at this stage is that several harmonics of the fundamental CDW must be present with appreciable amplitudes in the $1T_2$ phase. These harmonics, however, become extremely weak, to the point of being almost unmeasurable, in the $1T_1$ phase.

Our results for the $1T_2$ phase are consistent with a theoretical treatment recently developed on the basis of McMillan's free energy.[19] In this treatment use is made of the notion that domain boundaries are formed (called "discommensurations" by McMillan[20]), across which CDW phases are discontinuous. No numerical estimates, however, are given in Ref. 19 for the expected amplitudes of the harmonics.

The concept of discommensuration is more extensively developed in another paper,[21] dealing exclusively with the presence of harmonics in the incommensurate phase $1T_1$. While the numerical estimates for the ratios of higher-order to first-order satellites given in Ref. 21 are not out of line with the experimental observations, we feel that the higher-order satellites in the $1T_1$ phase can be understood without invoking the presence of CDW harmonics. For one thing, the experimental data are scarce. Most higher-order satellites simply disappear in the $1T_1$ phase. The only satellite we were able to measure (satellite D in Table II) can be reasonably explained on the basis of the simple sinusoidal model.

IV. CONCLUSIONS

The incommensurate CDW ($1T_1$) and noncommensurate ($1T_2$) phases of $1TaS_2$ have been investigated in detail using precession photography and counter measurements. It is found that uncontrollable temperature-dependent domains formation in the $1T_2$ phase prevents quantitative studies of the CDW satellites. No statement, therefore, can be made in this region about the phason temperature factor, whose existence and numerical value could instead be determined for the $1T_1$ phase.

Second- and higher-order satellites are found to be present in the $1T_2$ phase with intensities several orders of magnitude greater than the values predicted by the simple sinusoidal model for CDW's. It is suggested that higher-order harmonics of the fundamental CDW's are present in this phase. These harmonics, however, disappear in the $1T_1$ phase, in which the simple sinusoidal model is well applicable.

ACKNOWLEDGMENTS

The authors are deeply indebted to Professor A. W. Overhauser, who suggested many key ideas for interpreting our results. This work has been supported by the National Science Foundation Materials Research Laboratory Program Grant No. DMR-80-20249.

---

*Present address: National Synchrotron Light Source, Brookhaven National Laboratory, Upton, NY 11973.

[1]A preliminary report on this work has been presented in Ref. 14.

[2]A. W. Overhauser, Phys. Rev. B **3**, 3173 (1971).

[3]D. E. Moncton, J. D. Axe, and F. J. Di Salvo, Phys. Rev. B **16**, 801 (1977).

[4]H. Cailleau, F. Moussa, C. M. E. Zeyen, and J. Bouillot, Solid State Commun. **33**, 407 (1980).

[5]L. Bernard, R. Currat, P. Delamoye, C. M. E. Zeyen, S. Hubert, and R. de Kouchkovsky, J. Phys. C **16**, 433 (1983).

[6]J. W. Lynn, M. Izumi, G. Shirane, S. A. Werner, and R. B. Saillant. Phys. Rev. B **12**, 1154 (1975).

[7]C. B. Scruby, P. M. Williams, and G. S. Parry, Philos. Mag. **31**, 225 (1975).

[8]A. H. Thompson, F. R. Gamble, and J. F. Revelli, Solid State Commun. **9**, 981 (1971).

[9]See, for example, F. Lévy, Il Nuovo Cimento, **38B**, 359 (1977).

[10]*International Tables for X-Ray Crystallography* (Kynoch, Birmingham, England, 1974), Vol. IV.

[11]See, for example, R. W. James, *The Optical Principles of the Diffraction of X Rays* (Cornell University Press, Ithaca, 1965), Chap. VI, Sect. 3-d.

[12]R. Moret and R. Colella, Solid State Commun. **38**, 1175 (1981).

[13]Since the crystal thickness could not be assumed to be infinite, the dynamical integrated intensity was calculated by numerical integration of form 3.137 in Ref. 22.

[14]L. D. Chapman and R. Colella, Phys. Rev. Lett. **52**, 652 (1984).

[15]G. F. Giuliani and A. W. Overhauser, Phys. Rev. B **26**, 1660 (1982).

[16]The atomic scattering factors have been calculated using an analytical formula given in Ref. 23. The anomalous dispersion corrections were taken from Ref. 24.

[17]J. D. Axe, Phys. Rev. B **21**, 4181 (1980).

[18]A. Hogervorst, W. J. A. M. Peterse, and P. M. de Wolff, in *Modulated Structures—1979 (Kailua Kona, Hawaii),* Proceedings of the International Conference on Modulated Structures, edited by J. M. Cowley, J. B. Cohen, M. B. Salamon, and B. J.

Wuensch (AIP, New York, 1979), pp. 217–219.
[19]K. Nakanishi, J. Takatera, Y. Yamada, and H. Shiba, J. Phys. Soc. Jpn. **43**, 1509 (1977).
[20]M. L. McMillan, Phys. Rev. B **14**, 1496 (1976).
[21]K, Nakanishi and H. Shiba, J. Phys. Soc. Jpn. **43**, 1839 (1977).
[22]W. H. Zachariasen, *Theory of X-Ray Diffraction in Crystals* (Wiley, New York, 1945).
[23]D. T. Cromer and J. B. Mann, Acta Crystallogr. Sect. A **24**, 321 (1968).
[24]D. T. Cromer and D. Liberman, J. Chem. Phys. **53**, 1891 (1970).

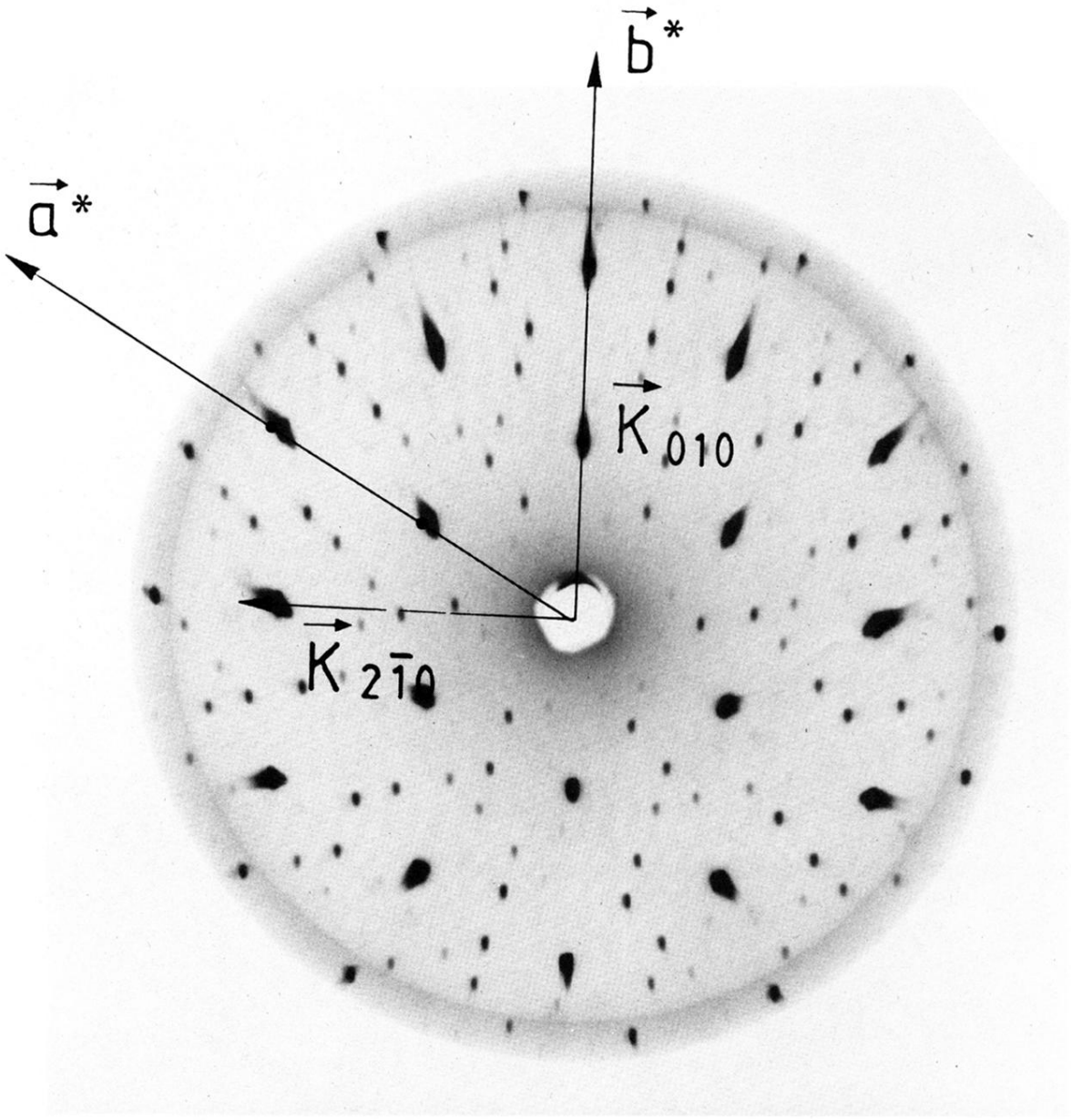

FIG. 1. Precession photograph of the (h k 0) layer at room temperature. Mo $K\alpha$ radiation. The heavy spots are Bragg reflections. Only second- and higher-order satellites are visible in this photograph.

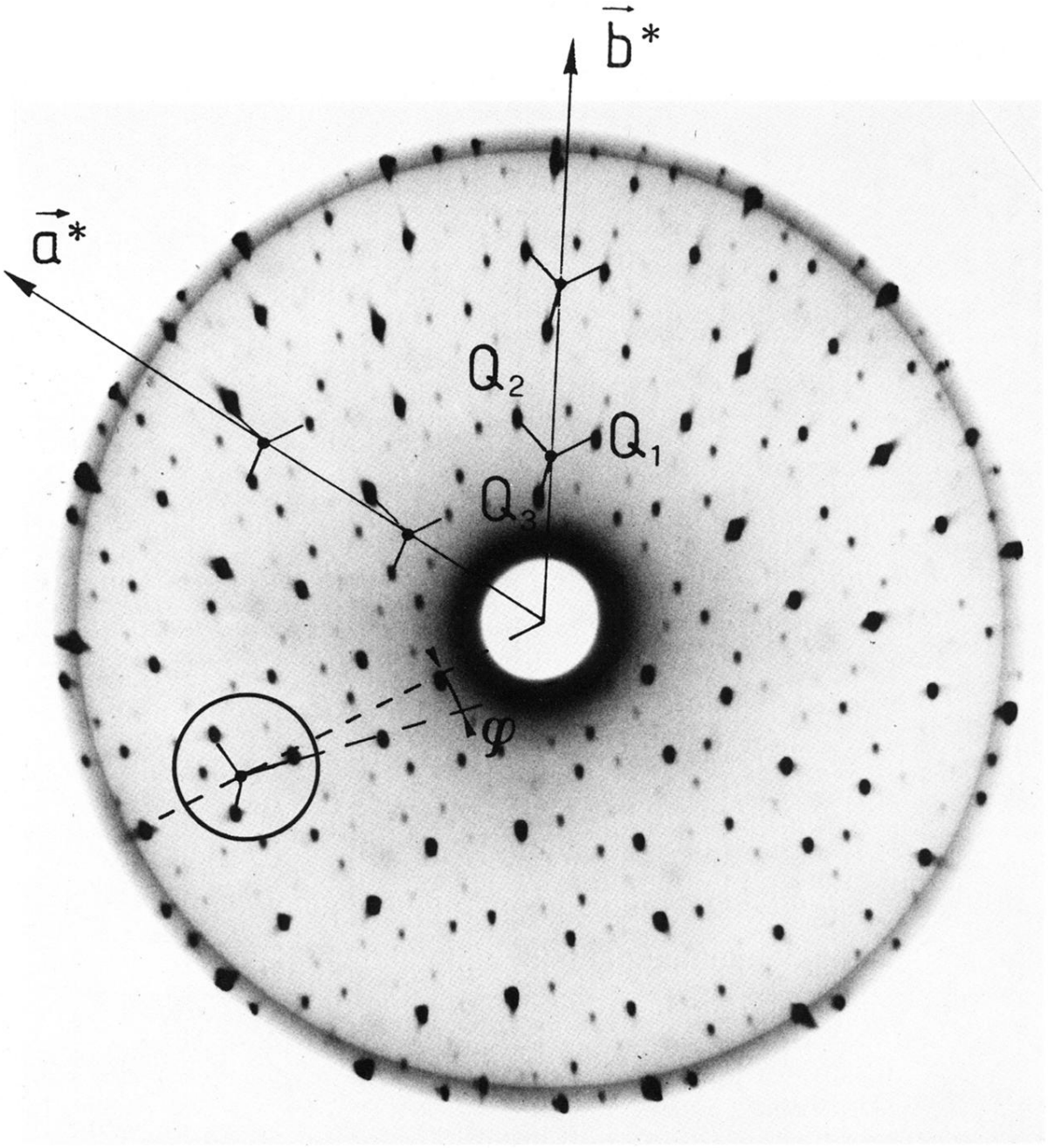

FIG. 2. Precession photograph of the (h k $\frac{1}{3}$) layer at room temperature. The triplet enclosed by a black circle (heavy spots) corresponds to a set of three first-order satellites associated with the (020) Bragg reflection. Higher-order satellites (up to third order) are visible.

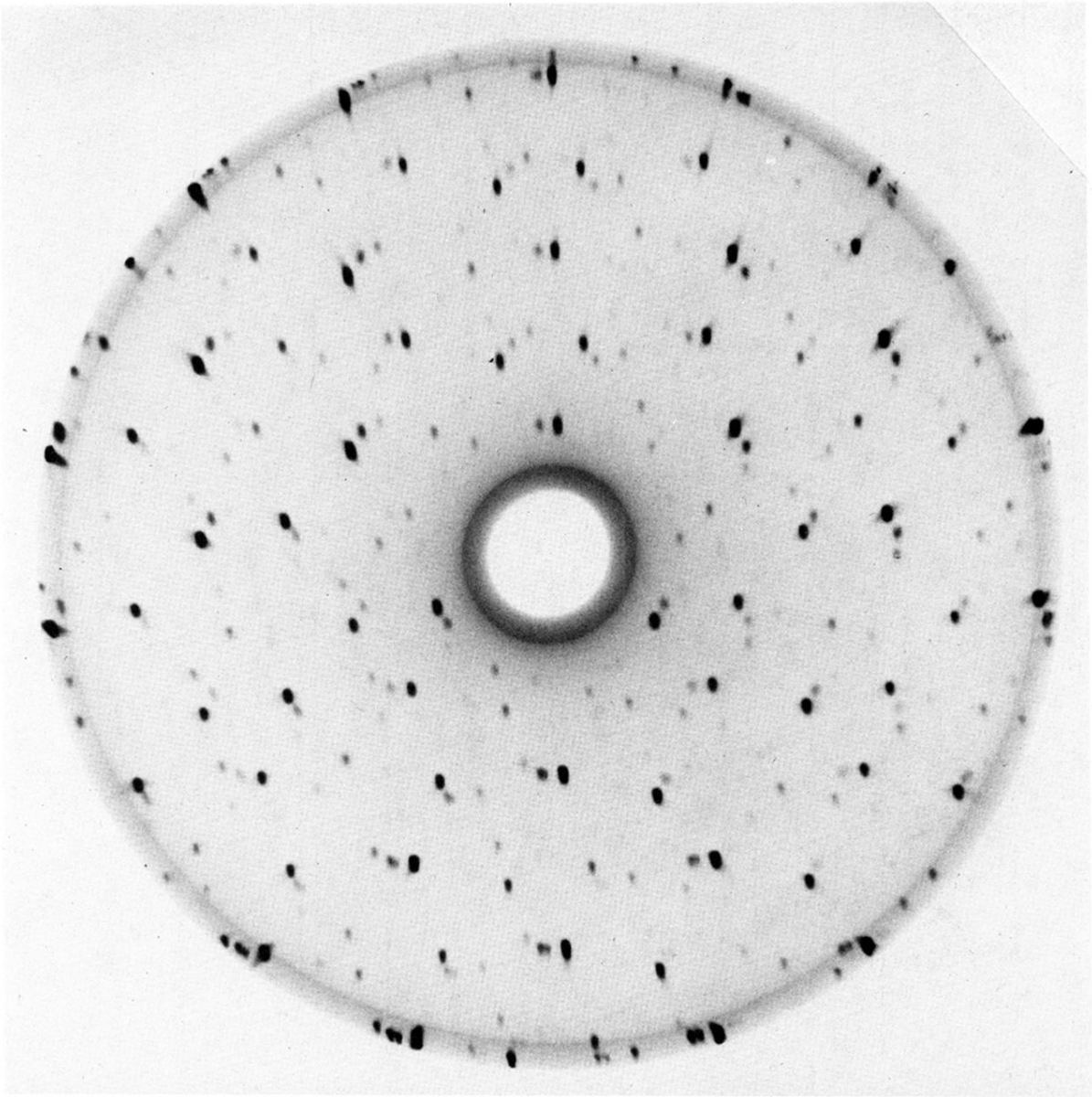

FIG. 3. Same as Fig. 2, except that $T = 50\,^{\circ}\mathrm{C}$. Two sets of spots are visible, corresponding to two equivalent sets of CDW satellites, with opposite orientations around the c axis with respect to the main reciprocal lattice.

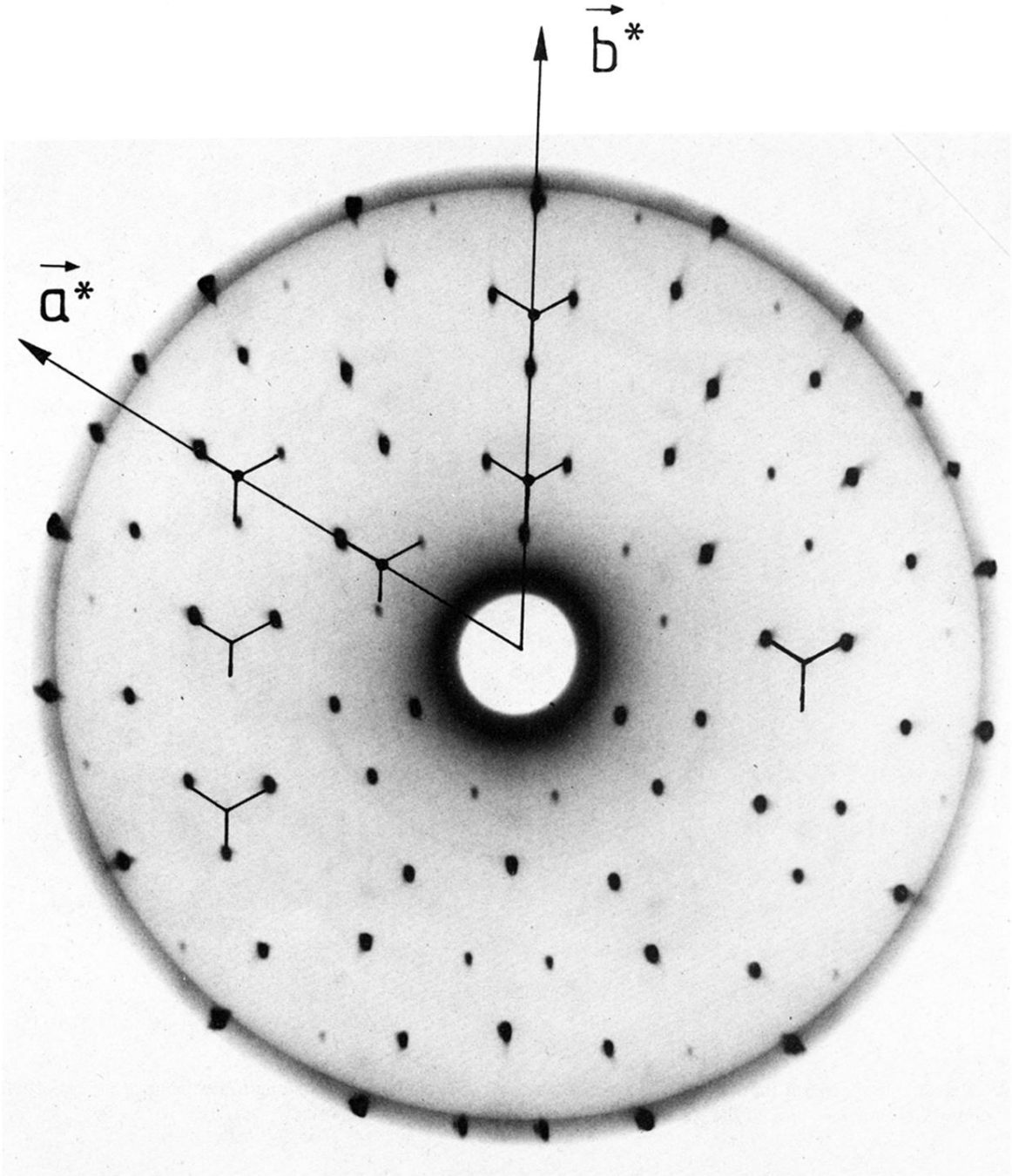

FIG. 4. Same as Fig. 2, except that $T=70\,^{\circ}\mathrm{C}$. Only first-order satellites are visible here. The crystal is still in $1T_2$ phase, but the CDW satellites system exhibits features that are typical of the $1T_1$ phase.

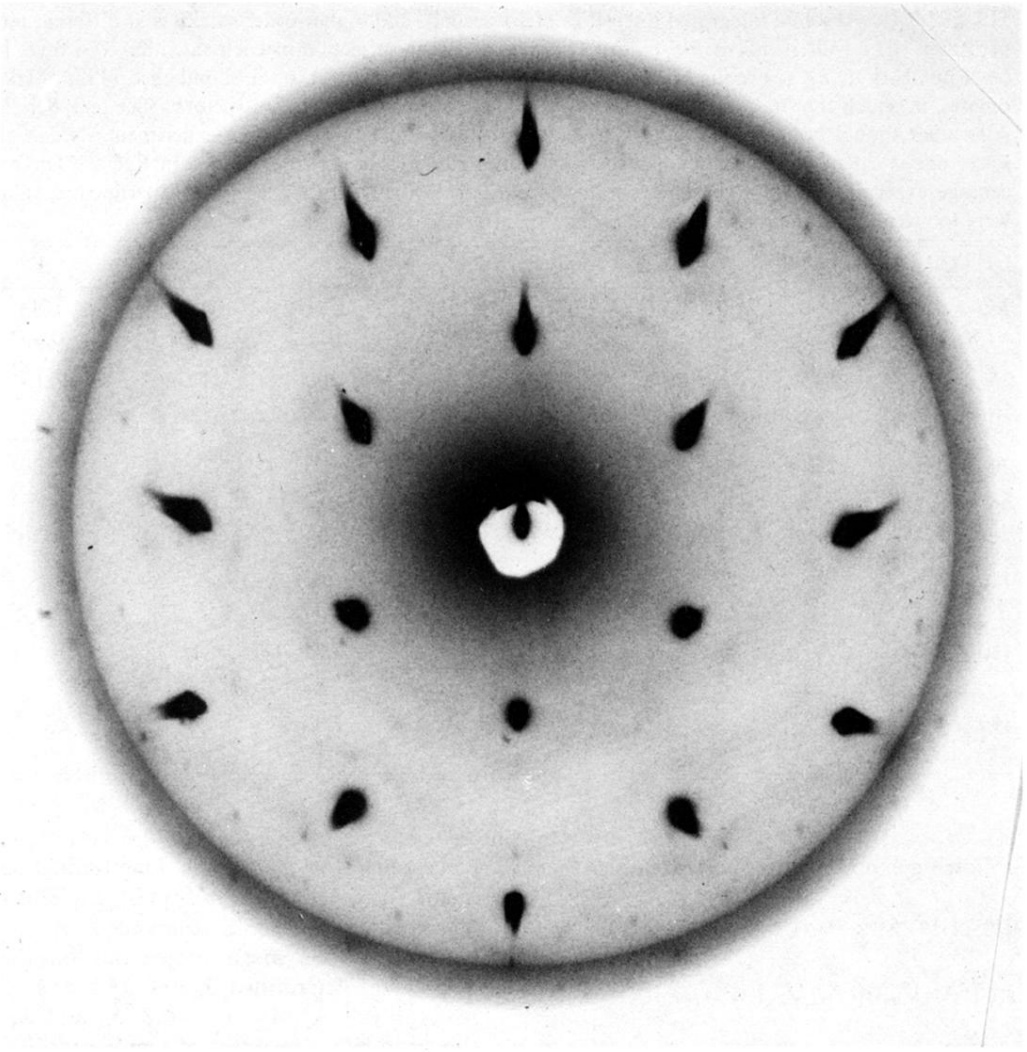

FIG. 5. Same as Fig. 4, except that here the (h k 0) plane is shown. No more satellites are visible, and the thermal diffuse scattering has increased.